

Shape transitions of metastable surface nanostructures

D. J. Vine, D. E. Jesson,* and M. J. Morgan
School of Physics, Monash University, Victoria 3800, Australia

V. A. Shchukin† and D. Bimberg
Institut für Festkörperphysik, Technische Universität Berlin, D-10623 Berlin, Germany

(Received 15 August 2005; revised manuscript received 21 September 2005; published 9 December 2005)

A shape transition between surface nanostructures which, as a function of island size, are associated with minima in formation energy per atom is modeled using a Fokker-Planck equation. We find that metastable states, associated with positive gradients in island chemical potential, can dominate the dynamics of the transition. The resulting bimodal island size distribution function is metastable to Ostwald ripening which has important implications for the self-organization of quantum dots.

DOI: [10.1103/PhysRevB.72.241304](https://doi.org/10.1103/PhysRevB.72.241304)

PACS number(s): 81.07.Ta, 68.35.Md, 68.65.-k, 81.16.-c

The self-assembly and self-organization of nanostructures on surfaces can be utilized to produce quantum dot arrays for device applications.^{1,2} This can be readily achieved, for example, by depositing thin films using deposition techniques such as molecular beam epitaxy.³⁻⁵ The resulting islands, or dots, can be overgrown by appropriate layers to form the basis for devices such as semiconductor lasers. However, size uniformity is critical for many applications which has led to significant efforts to understand the key factors governing the coarsening of quantum dot arrays.

Surface nanostructures that possess a minimum in formation energy per atom (MEA) as a function of island size (MEA systems) are particularly attractive candidates for device applications because they are associated with a thermodynamically favored size. By simply annealing such structures, one might anticipate the creation of arrays with good size uniformity. Although it is not possible to identify MEA systems *a priori*, theoretical studies have shown that coherently strained two-dimensional (2D) islands,⁶⁻⁸ three-dimensional (3D) islands with surface stress discontinuities at their edges^{9,10} or 3D islands with strain renormalized surface energy^{9,11} are potential candidates for MEA systems.

A feature of particular interest in the case of 3D nanostructures is the possibility that surface islands can undergo shape transitions.¹²⁻²³ This can result in a multimodal island size distribution function during the self-organization of quantum dot systems that can deleteriously influence device performance. Understanding the dynamics of shape transitions is therefore of critical importance to control island size distributions and obtain good size uniformity.

Theoretical descriptions of quantum dot systems undergoing shape transitions can be broadly classified as being thermodynamic or kinetic in nature. Kinetic models have emphasized the discontinuity in island chemical potential as islands attain a critical transition size.¹² Upon transformation to a new shape, the lower chemical potential islands grow rapidly, resulting in a bimodal size distribution. In contrast, thermodynamic models associate peaks in the island size distribution function with minima in formation energy per atom for different island shapes.^{13,15,17} However, as discussed by Rudd *et al.*,¹⁵ the dynamics of the transition between “stable”

states in thermodynamic models and the consequences for self-organization are relatively unexplored.

In this Rapid Communication, we therefore develop a theoretical description of shape transition dynamics in MEA systems. Surprisingly, metastable states, associated with positive gradients in chemical potential, are found to dominate the dynamics of the transition. These states are distinct from energy per atom minima and have important implications for self-organization of MEA systems and the application of thermodynamic models to interpret experimental data.^{13,15,17}

To model a shape transition between nanostructures exhibiting MEA behavior we consider the specific case of 3D semiconductor islands with strain-renormalized surface energy which are assumed to exhibit MEA properties.^{9,11} The dimensionless formation energy $E_s(N)$ of a faceted quantum dot as a function of the number of atoms N it contains is given by^{9,11}

$$E_s(N) = -\alpha_s N + \beta_s N^{2/3} - 2N^{1/3} \ln(e^{1/2} N^{1/3}). \quad (1)$$

The first term is the island relaxation energy, the second term incorporates the change in renormalized surface energy due to island formation, and the third term combines the positive short range energy of the island edges with the negative surface stress induced elastic relaxation energy at the edges, $\Delta E_{elastic}^{edges}$. The parameter α_s is the ratio of the volume relaxation energy to $|\Delta E_{elastic}^{edges}|$ and β_s is the ratio of the renormalized surface energy to $|\Delta E_{elastic}^{edges}|$. The subscript $s=1, 2$ of the parameters α_s, β_s , refers to two different nanostructure shapes. We assume that the island array is sufficiently dilute so that the elastic interaction between islands can be neglected.

Quantitative values of the parameters α_s, β_s are presently unknown. For the purpose of this simulation we assume the arbitrary but physically reasonable values of $\alpha_1=4.2$, $\beta_1=-0.8$, $\alpha_2=5.2$ and $\beta_2=0.0$. In Fig. 1(a) we plot the island formation energy per atom $\epsilon_s(N)=E_s(N)/N$ as a function of island size for two shapes 1 and 2. Each shape is associated with a minimum in $\epsilon_s(N)$ at $\epsilon_1(N_1^E)$ and $\epsilon_2(N_2^E)$. For small island sizes, shape 1 is energetically favorable. However,

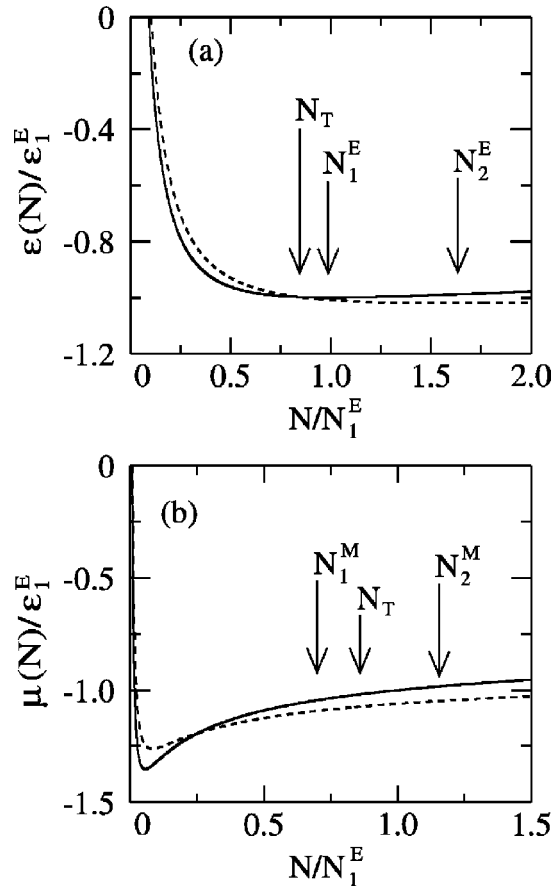


FIG. 1. (a) Energy per atom $\epsilon_s(N)$ and (b) chemical potential $\mu_s(N)$ plotted as a function of N/N_1^E for island shapes 1 (solid line) and 2 (dashed line). Minima in $\epsilon_s(N)$ occur at N_1^E, N_2^E for shapes 1 and 2, respectively. Shape 1 will transform into shape 2 at N_T . Chemical potentials of islands 1 and 2 have minima at N_1^M, N_2^M , respectively.

shape 2 is energetically preferred for large island sizes and shape 1 will transform into shape 2 at N_T where $\epsilon_1(N_T) = \epsilon_2(N_T)$. Here we have specifically considered the interesting case where shapes 1 and 2 have minima in $\epsilon_s(N)$. However, other parametrizations are also possible that, for example, include transitions between shapes with, and without, minima in $\epsilon_s(N)$.

In standard thermodynamic models, one might anticipate peaks in the island size distribution associated with the two energy per atom minima present in Fig. 1(a). However, the dynamical evolution of an island array towards the equilibrium distribution depends on the island chemical potential $\mu_s(N) = dE_s(N)/dN$ given by

$$\mu_s(N) = -\alpha_s + \frac{2}{3}\beta_s N^{-1/3} - \frac{2}{3}N^{-2/3} \ln(e^{3/2}N^{1/3}). \quad (2)$$

Figure 1(b) displays the chemical potentials of island shapes 1 and 2 with minima at N_1^M and N_2^M , respectively. We note that the chemical potential minima occur at island sizes that are appreciably smaller than the sizes corresponding to the minima in $\epsilon_s(N)$. This is a general feature for 3D islands with

energetics of the form given by Eq. (1) for a wide range of α_s, β_s parameter space¹¹ and has important implications for the self-organization of MEA systems.

To model the shape transition of the 3D strained island array we use the Fokker-Planck equation which is derived as an approximation of the kinetic Becker-Döring model for the aggregation of particles.²⁴ This equation has been used to study time-dependent nucleation theory²⁵ and the evolution of nanostructure arrays.²⁶ It can be viewed as an extension of standard coarsening theory^{27–32} with the important addition of a thermal broadening term which is significant at high temperatures and/or when the island size distribution width is narrow. If $f(t, N)$ is the island size distribution function such that $f(t, N)dN$ specifies the number of islands per unit area containing atoms between N and $N+dN$ at time t , then the appropriate dimensionless Fokker-Planck equation governing the time evolution of the islands is

$$\frac{\partial f(t, N)}{\partial t} = -\frac{\partial}{\partial N} J(t, N). \quad (3)$$

The island flux through islands of size N is given by

$$J(t, N) = \omega(N) \left(\frac{\bar{\mu} - \mu(N)}{\Theta} f(t, N) - \frac{\partial}{\partial N} f(t, N) \right), \quad (4)$$

where $\Theta = k_B T$ is a scaled effective temperature. A standard case is considered where mass transfer is limited by attachment (detachment) processes to (from) the island perimeter¹² and $\omega = N^{1/3}$ for appropriate scaling of the units of time. The first term in Eq. (4) is conventionally referred to as the drift contribution and the second term as the diffusion contribution. The drift velocity is defined as

$$u(t, N) = \omega(N) \left[\frac{\bar{\mu} - \mu(N)}{\Theta} \right]. \quad (5)$$

The mean-field chemical potential $\bar{\mu}$ is determined from the constraint that the island flux $J(t, N)$ integrated over all islands is equal to the deposition flux Φ .

To illustrate the salient features of a shape transition within a MEA system we simulate a growth and anneal experiment at the scaled effective temperature $\Theta = 1$. The initial distribution at $t=0$ is located within the range $N_1^C < N < N_T$ as shown in Fig. 2 and consists entirely of shape 1 islands. This could be taken to mimic the distribution resulting from nucleation, for example. The evolution of $f(t, N)$ is obtained by solving Eq. (3) numerically and the mean-field chemical potential $\bar{\mu}$ evaluated after each time increment.

The initial distribution is subjected to a deposition flux $\Phi = 500$ (in scaled units) which moves the mean island size to a larger value. A transition from shape 1 to shape 2 occurs as the main distribution of shape 1 islands reaches N_T . At $t = 1680$, a second peak consisting entirely of shape 2 islands begins to form at $N \approx 1.3N_1^E$ resulting from a small but significant flux of islands across the intervening size space. During the transition from shape 1 to shape 2, shape 2 islands are associated with an abrupt decrease in chemical potential due to the discontinuous transition between chemical potential curves in Fig. 1(b) at $N = N_T$. These islands then grow rapidly as $\mu_2(N) < \bar{\mu}$ resulting in a bifurcation of the island size dis-

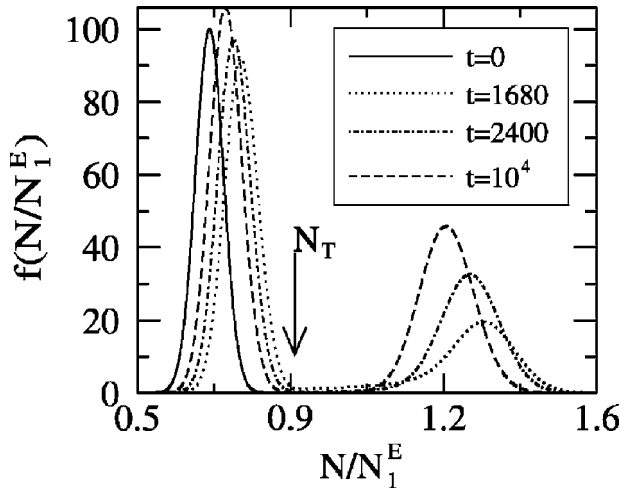


FIG. 2. Island size distribution function $f(N/N_1^E)$ evolving with time t (scaled units). Shape 1 transforms into shape 2 at N_T .

tribution and a second peak centred on $N=1.3N_1^E$. It is important to note that the distribution at $t=1680$ has not significantly broadened from the initial distribution at $t=0$, which is unexpected from standard coarsening theory.^{27–32} This can be attributed to the positive chemical potential gradient in this regime. To explain the absence of broadening we consider a drift-dominated regime and zero deposition flux. The mean-field chemical potential $\bar{\mu}$ is a weighted mean of the island chemical potentials over the island size distribution. With a positive chemical potential gradient, small islands with $\mu_1(N) < \bar{\mu}$ grow while large islands with $\mu_1(N) > \bar{\mu}$ shrink [see Eq. (5)]. Therefore, the drift term causes the distribution to narrow about the mean island size. This can be regarded as “inverse Ostwald ripening.” Eventually, this is opposed by the diffusion term until the two terms become approximately equal in magnitude but opposite in sign. This results in a long-lived transient or metastable state.³³ If growth is “close to equilibrium” such that $\bar{\mu}$ is only slightly increased by the deposition flux, then the metastable state will dominate the island size distribution at a particular coverage and the state will simply drift to higher island volumes with minimal broadening of the profile as illustrated in Fig. 2.

The metastable nature of these as-grown island distributions is emphasized during postgrowth annealing. Upon turning off the deposition flux at $t=2000$, the peaks of the bimodal island size distribution function associated with shapes 1 and 2 evolve towards metastable states at $t=2400$, as illustrated in Fig. 2. At $t=10^4$, these states are extremely slowly evolving and our simulations indicate that the bimodal distribution is stable against ripening on experimentally relevant time scales. This metastable bimodal distribution is the direct result of a dynamic cancellation of the drift and diffusion terms in Eq. (4). It is attained before, and is distinct from, the equilibrium distribution associated with the energy minima in Fig. 1(a). The two metastable states are approximately Gaussian shapes centered on N_1^M and N_2^M . This is expected if we note that, to a good approximation, we may approximate

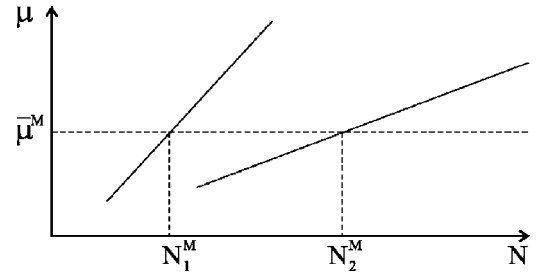


FIG. 3. Construction linking the mean-field chemical potential $\bar{\mu}^M$ with the chemical potentials of the two shapes, $\mu_1(N_1^M)$ and $\mu_2(N_2^M)$. In the linear approximation, the chemical potential variation of the two shapes is approximated by straight lines of different slope.

the variation of $\mu_s(N)$ over the width of each distribution as straight lines of positive gradient.^{33,34} If the mean-field chemical potential $\bar{\mu}^M = \mu_s(N_s^M)$ then the chemical potential at size N can be written as $\mu_s(N) = (N - N_s^M)d\mu_s/dN + \mu_s(N_s^M)$. Inserting this linear form into Eq. (4) and looking for steady-state solutions where $J(t, N) = 0$ yields,

$$f_s^M(N) = A_s^M \exp\left(-\frac{d\mu_s(N - N_s^M)^2}{dN \cdot 2\Theta}\right), \quad (6)$$

where A_s^M is a constant. This Gaussian distribution function, centered on N_s^M , can also be viewed as the equilibrium Gibbs-Boltzmann distribution associated with a linear chemical potential variation. Given that the shape transition is associated with two curves of positive chemical potential gradient, the condition for metastability, in the linear potential approximation, is given by $\mu_1(N_1^M) = \mu_2(N_2^M) = \bar{\mu}^M$, which is schematically represented by the construction in Fig. 3. The standard deviation of the Gaussian distribution approximating each metastable state is given from Eq. (6) by $\sigma_s = [\Theta/(d\mu_s/dN)]^{1/2}$.^{33,34} Consequently, $\sigma_2 > \sigma_1$, in agreement with Fig. 2, since $[d\mu_1/dN]_{N_1^M} > [d\mu_2/dN]_{N_2^M}$ [Fig. 1(b)].

In summary, we have presented a theory based on the Fokker-Planck equation that incorporates island shape transitions in MEA systems. Long-lived transient states, which are distinct from the energy per atom minima in MEA systems, can dominate the dynamics of the transition. The system stagnates into a bimodal distribution which is metastable to Ostwald ripening. This unusual kinetics has important implications for the self-organization of MEA systems. It is important to appreciate the full ramifications of thermodynamic models and, in particular, the existence of metastable states when applying them to interpret the evolution of quantum dot systems in which shape transitions are observed.^{13,15,17}

V.A.Sh. and D.B. are grateful to the Deutsche Forschungsgemeinschaft (Sfb 296), the BMBF, and SANDiE Network of Excellence of the European Commission, Contract No. NMP4-CT-2004-500101. V.A. Sh. acknowledges support from the Russian Foundation for Basic Research. D.E.J. acknowledges support from the ARC.

*Electronic address: david.jesson@sci.monash.edu.au

†On leave from A. F. Ioffe Physical Technical Institute, St. Petersburg 194021, Russia.

- ¹D. Bimberg, M. Grundmann, and N. N. Ledentsov, *Quantum Dot Heterostructures* (Wiley, Chichester, 1998).
- ²V. A. Shchukin, N. N. Ledentsov, and D. Bimberg, *Epitaxy of Nanostructures* (Springer, Heidelberg, 2003).
- ³D. Leonard, K. Pond, and P. M. Petroff, Phys. Rev. B **50**, 11687 (1994).
- ⁴J. M. Moison, F. Houzay, F. Barthe, L. Leprince, E. Andre, and O. Vatel, Appl. Phys. Lett. **64**, 196 (1994).
- ⁵N. P. Kobayashi, T. R. Ramachandran, P. Chen, and A. Madhukar, Appl. Phys. Lett. **68**, 3299 (1996).
- ⁶V. I. Marchenko, JETP Lett. **33**, 381 (1981).
- ⁷D. Vanderbilt, Surf. Sci. **268**, L300 (1992).
- ⁸K. O. Ng and D. Vanderbilt, Phys. Rev. B **52**, 2177 (1995).
- ⁹V. A. Shchukin, N. N. Ledentsov, P. S. Kop'ev, and D. Bimberg, Phys. Rev. Lett. **75**, 2968 (1995).
- ¹⁰F. Liu, Phys. Rev. Lett. **89**, 246105 (2002).
- ¹¹T. P. Munt, D. E. Jesson, V. A. Shchukin, and D. Bimberg, Appl. Phys. Lett. **85**, 1784 (2004).
- ¹²F. M. Ross, J. Tersoff, and R. M. Tromp, Phys. Rev. Lett. **80**, 984 (1998).
- ¹³G. Medeiros-Ribeiro, A. M. Bratkovski, T. I. Kamins, D. A. A. Ohlberg, and R. S. Williams, Science **279**, 353 (1998).
- ¹⁴F. M. Ross, R. M. Tromp, and M. C. Reuter, Science **286**, 1931 (1999).
- ¹⁵R. E. Rudd, G. A. D. Briggs, A. P. Sutton, G. Medeiros-Ribeiro, and R. S. Williams, Phys. Rev. Lett. **90**, 146101 (2003).
- ¹⁶J. A. Floro, G. A. Lucadamo, E. Chason, L. B. Freund, M. Sinclair, R. D. Twisten, and R. Q. Hwang, Phys. Rev. Lett. **80**, 4717 (1998).
- ¹⁷R. J. Wagner and E. Gulari, Surf. Sci. **590**, 1 (2005).
- ¹⁸See for example, A. Rastelli, M. Stoffel, J. Tersoff, G. S. Kar, and O. G. Schmidt, Phys. Rev. Lett. **95**, 026103 (2005), and the references contained therein.
- ¹⁹T. Hammerschmidt and P. Kratzer, in *Proc. 27th Int. Conf. Phys. Semicon.*, edited by J. Menéndez and C. G. V. de Walle (2004), p. 601.
- ²⁰M. C. Xu, Y. Temko, T. Suzuki, and K. Jacobi, Phys. Rev. B **71**, 075314 (2005).
- ²¹K. Pötschke, L. Muller-Kirsch, R. Heitz, R. L. Sellin, U. W. Pohl, D. Bimberg, N. Zakharov, and P. Werner, Physica E **21**, 606 (2004).
- ²²G. Costantini, C. Manzano, R. Songmuang, O. G. Schmidt, and K. Kern, Appl. Phys. Lett. **82**, 3194 (2003).
- ²³G. Costantini, A. Rastelli, C. Manzano, R. Songmuang, O. G. Schmidt, K. Kern, and H. von Känel, Appl. Phys. Lett. **85**, 5673 (2004).
- ²⁴J. L. Velázquez, J. Stat. Phys. **92**, 195 (1998).
- ²⁵J. W. Christian, *The Theory of Transformations in Metals and Alloys, Part I* (Pergamon Press, New York, 2002).
- ²⁶E. M. Lifshitz and L. P. Pitaevskii, *Physical Kinetics* (Butterworth-Heinemann, Oxford, 1981).
- ²⁷I. M. Lifshitz and V. V. Slyozov, J. Phys. Chem. Solids **19**, 35 (1961).
- ²⁸B. K. Chakraverty, J. Phys. Chem. Solids **28**, 2401 (1967).
- ²⁹H. A. Atwater and C. M. Yang, J. Appl. Phys. **67**, 6202 (1990).
- ³⁰D. E. Jesson, T. P. Munt, V. A. Shchukin, and D. Bimberg, Phys. Rev. B **69**, 041302(R) (2004).
- ³¹P. W. Voorhees, Annu. Rev. Mater. Sci. **22**, 197 (1992).
- ³²M. Zinke-Allmann, L. C. Feldman, and M. H. Grabow, Surf. Sci. Rep. **16**, 377 (1992).
- ³³D. E. Jesson, T. P. Munt, V. A. Shchukin, and D. Bimberg, Phys. Rev. Lett. **92**, 115503 (2004).
- ³⁴D. E. Jesson, Trans. R. Soc. S. Afr. **58**, 141 (2003).